Structural Engineering and Mechanics, *Vol. 51, No. 1 (2014) 131-140*
DOI: http://dx.doi.org/10.12989/sem.2014.51.1.131

Rational analysis model and seismic behaviour of tall bridge piers

Jianzhong Li[1a], Zhongguo Guan[*1] and Zhiyao Liang[2b]

[1]*Department of Bridge Engineering, Tongji University, Shanghai, P.R. China*
[2]*Engineering Management Office, Suzhou Industrial Park, Suzhou, P.R. China*

(Received April 7, 2011, Revised May 9, 2014, Accepted May 18, 2014)

Abstract. This study focuses on seismic behaviour of tall piers characterized by high slender ratio. Two analysis models were developed based on elastic-plastic hinged beam element and elastic-plastic fiber beam element, respectively. The effect of the division density of elastic-plastic hinged beam element on seismic demand was discussed firstly to seek a rational analysis model for tall piers. Then structural seismic behaviour such as the formation of plastic hinges, the development of plastic zone, and the displacement at the top of the tall piers were investigated through incremental dynamic analysis. It showed that the seismic behaviour of a tall pier was quite different from that of a lower pier due to higher modes contributions. In a tall pier, an additional plastic zone may occur at the middle height of the pier with the increase of seismic excitation. Moreover, the maximum curvature reaction at the bottom section and maximum lateral displacement at the top turned out to be seriously out of phase for a tall pier due to the higher modes effect, and thus pushover analysis can not appropriately predict the local displacement capacity.

Keywords: tall pier; analysis model; seismic behaviour; higher-mode effect; displacement capacity

1. Introduction

Recently, many highways and railways have been built at west China with the rapid development of local economy. Because most of the area is mountainous terrain, a high percentage of bridges have to be used; in some area, the total length of bridges even exceeds 30 percent length of a whole road. It is showed that most of these bridges are constructed in continuous girder bridges or frame bridges. However, these bridges are quite different from those built on plain terrain; in order to span some deep valleys, nearly 40 percent bridges have a pier height exceeding 40 m, some of them even higher than 100 m. For instance, the Luohe Highway Bridge in China has a highest pier about 143 m and that of the Huatupo Railway Bridge is about 110 m. These high piers usually have a very high slender ratio, and this definitely changes the dynamic characteristics of the whole structure and subsequently results in a different structural performance under earthquake action. Moreover, most of the mountainous areas in west China are high seismic zones.

∗Corresponding author, Associate Professor, E-mail: guanzhongguo@tongji.edu.cn
[a]Professor, E-mail: lijianzh2011@163.com
[b]Senior Engineer, E-mail: lizhiyao@163.com

http://www.techno-press.org/?journal=sem&subpage=8 ISSN: 1225-4568 (Print), 1598-6217 (Online)

Therefore, the seismic response analysis and rational design measures for these high pier bridges become a major concern.

During the past three decades, considerable experimental and theoretical researches on seismic behaviour of girder bridges have been carried out (Kowalsky 2000, Fan 2007, Priestley *et al*. 1996, 2007). Some useful seismic design strategy, such as ductility or displacement design method, capacity design method and so on, have been presented and also wildly used, even accepted by some design codes. However, most of them are towards conventional bridges. In newly revised Guidelines for Seismic Design of Highway Bridges (JTG/T B02-01-2008 2008) in China, it is required the maximum pier height not exceed 40 m, or specified research work need to be conducted. Although no pier height limit is clearly specified in the AASHTO Guide Specifications for LRFD Seismic Bridge Design (2007), it should only be taken to apply to normal bridges. Actually, it has been verified that the conventional seismic design method can not correctly predict the seismic performance for tall buildings or chimney (Tsai *et al*. 2002, Gould *et al*. 2006, Poursha *et al*. 2009). Memari *et al*. (2010) evaluated an elevated highway bridge in a low seismic region through linearly elastic analysis. Ceravolo *et al*. (2009) investigated a bridge with tall piers and pointed out pier dynamics would govern the seismic behaviour and the current design strategy proved to be inadequate. Li *et al*. (2005) compared the seismic behaviour of lower and tall piers and concluded that both seismic demand and capacity of tall piers were quite different from lower piers due to the higher modes effect on seismic response. Bu *et al*. (2012) also discussed the seismic performance of precast segmental tall bridge columns.

This study focuses on the seismic behaviour of tall piers, in particular higher modes effect. To properly capture the special dynamic characteristics of tall piers, two nonlinear finite element models were introduced and compared, and also incremental dynamic analysis was conducted to investigate seismic behaviour of bridges with tall piers, from the initial elastic state to the ultimate limit state. Moreover, the validity of pushover analysis in determining local displacement capacity recommended in the code was also discussed for tall piers.

2. Analysis model

Two multi-span continuous deck highway bridges were investigated in this study, one with a

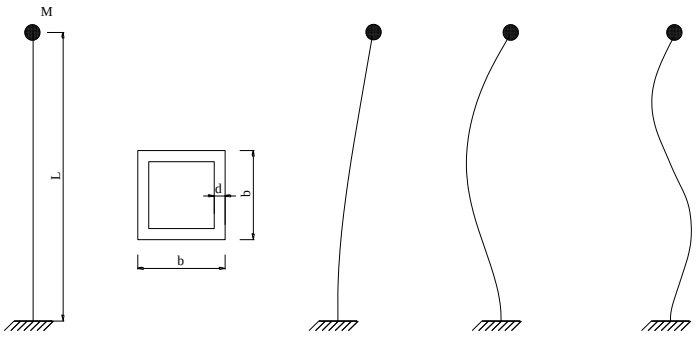

(a) analysis model (b) cross section (c) 1st mode (d) 2nd mode (e) 3rd mode

Fig. 1 Analysis model and structural configuration

Table 1 Basic parameters of piers

Height *L*/m	Length *b*/m	Thickness *d*/m	Superstructure mass *M*/t	Axial force ratio	Longitudinal steel ratio/%
30	3.2	0.4	700	0.096	1.48
90	4.4	0.5	700	0.092	1.48

Table 2 Natural periods and mass participation coefficients of piers

Height L/m	1st mode		2nd mode		3rd mode	
	Natural period/sec	Mass participation coefficient	Natural period/sec	Mass participation coefficient	Natural period/sec	Mass participation coefficient
30	1.225	0.872	0.103	0.089	0.040	0.026
90	4.093	0.685	0.552	0.171	0.201	0.058

height of 30 m for all piers representing a bridge with normal height piers and the other with a height of 90 m for all piers representing a typical tall pier bridge. Both of the two bridges were modeled as a cantilever beam with a lumped masses at nodes and an equivalent superstructure concentrate mass M at the top of the pier, as shown in Fig. 1. Detail structural information can be seen in Table 1. The natural periods and mass participation coefficients are shown in Table 2.

In order to capture the special dynamic characteristic of tall piers, particularly the contribution of high modes on the seismic response, and also to precisely simulate the nonlinear behaviour of pier elements, two types of finite element models were developed, based on inelastic hinged beam element using SAP2000 program and inelastic fiber beam element by Opensees platform, respectively. Inelastic hinged beam elements are commonly practiced in nonlinear analysis for frame structures, in which plastic deformation along the element is concentrated upon the rigid-plastic hinges at the ends of the element. In this model, effective flexural stiffness as defined in the AASHTO specification was used to account for the reduction of section flexural stiffness due to the cracking, and a typical yield surface of reinforced concrete proposed by Bresler *et al*. (1985) to determine the force deformation curve of the hinges. Besides, in order to investigate the effects of the element division density on seismic demands, the 30 m pier model is subdivided into 3, 5, 10, 15, 30 elements, and the 90 m pier model is subdivided into 3, 10, 20, 30, 45, 90 elements. Inelastic fibre beam elements have more elaborate nonlinear constitutive laws for each material (Silvia *et al*. 2005); therefore the model could yield more precise results in simulating the nonlinear hysteretic behavior of reinforced concrete frame members especially in seismic action. Recently, it becomes more and more noticeable (Taucer *et al*. 1991, Mohd Hisham 1994). In this model, the boxed RC sections are subdivided into confined concrete, unconfined concrete and longitudinal steel reinforcement fibers with perfect bond condition, and Mander's model (Mander *et al*. 1988) was presented in defining of stress-strain relationship for confined concrete and unconfined concrete and bilinear stress-strain relationship for longitudinal steel reinforcement, as shown in Fig. 2.

An ensemble of earthquake records (as shown in Table 3) are selected for considering the randomness of earthquake ground motions according to different seismic parameters, such as seismic magnitude, Peak Ground Acceleration (PGA) and predominant period. Predominant periods of selected earthquake records vary from 0.1 s to 0.92 s. Each record is scaled into 6

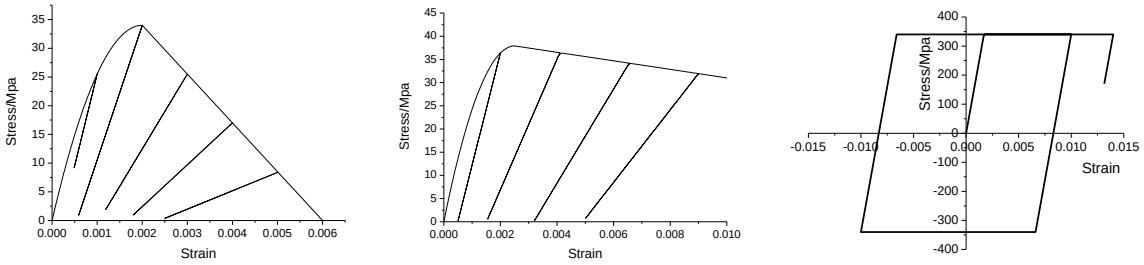

(a) unconfined concrete (b) confined concrete (c) steel reinforcement

Fig. 2 Material stress-strain relationship

Table 3 Earthquake records

Index	Earthquake Wave	Site	Magnitude	PGA/g	Predominant period/s
E1	1940 El Centro	Imperial Valley	7	0.313	0.46
E2	1995 Kobe	KJMA	6.9	0.821	0.34
E3	1971 San Fernando	Carbon Canyon Dam	6.6	0.071	0.26
E4	1989 Loma Prieta	Alameda Naval Air Stn Hanger	6.9	0.209	0.64
E5	Imperial Valley 1979	Westmorland Fire Station	5.5	0.171	0.1
E6	1999 Turkey	Ambarli	7.1	0.025	0.92
E7	Northridge 1994	Old Ridge Route	6.7	0.514	0.54
E8	Northridge 1994	Las Palmas	6.7	0.357	0.2
E9	Kern County 1952	Taft Lincoln School	7.4	0.178	0.44
E10	Tabas, Iran 1978	Tabas	7.4	0.852	0.2
E11	Hollister 1974	Hollister City Hall	5.2	0.177	0.3
E12	Tangshan 1976	Beijing Hotel	7.8	0.066	0.4

grades in PGA, from 0.2 g to 1.2 g, for a comprehensive incremental dynamic analysis (IDA) which is widely used recently to estimate structural performance under seismic loads more thoroughly (Vmvatsikos *et al*. 2002, Mander *et al*. 2007).

3. Seismic demands

3.1 Lower pier

In order to investigate the effect of the element division density on the plastic rotation demand for a lower pier, the plastic rotation demand for the 30 m pier with different element number subject to E6 earthquake wave is shown in Fig. 3. It is can be seen that only one plastic hinge appears at the bottom of the pier with 3 elements, but two or more plastic hinges appear at the bottom region with the increase of the element number.

Fig. 3 has shown that with the increase of the element division density, the plastic rotation of the plastic hinge at the bottom of the pier decreased due to multiple plastic hinges appears.

However, when the multiple plastic hinges appear the sum of plastic rotation for all plastic hinges with different elements keep nearly the same. The average plastic rotation with various element division densities subjected to 12 earthquakes scaling PGA from 0.2 g to 1.2 g is shown in Fig. 4.

From Fig. 3 and Fig. 4, if just one plastic hinge appears for the 30 m pier with 3 elements, the plastic rotation of this plastic hinge nearly equals to the sum of the plastic rotation with multiple plastic hinges, even severe earthquake excitation. When there are multiple plastic hinges along a pier, the sum of the plastic rotation for all plastic hinges should be represented the seismic plastic rotation demand for a pier. If the plastic rotation for plastic hinge at bottom of a pier is considered as the plastic rotation demand of the pier, it will be underestimated overly.

Top displacement is also an important index that computes the displacement ductility demand. The average displacement at the top of the pier with various analytical models subjected to 12 earthquakes scaling PGA from 0.2 g to 1.2 g is shown in Fig. 5. From Fig. 5, it can be seen that the displacement at the top of the pier with different analytical models are almost equivalent, even for analytical model with 3 elements.

Fig. 6 shows a plot of an instantaneous horizontal displacement and the plastic rotation values along the pier estimated by the elastic-plastic element model with 30 elements at time t=17.61 s. At the same time (t=17.61 s), the instant displacement and the plastic rotation for the 30 m pier

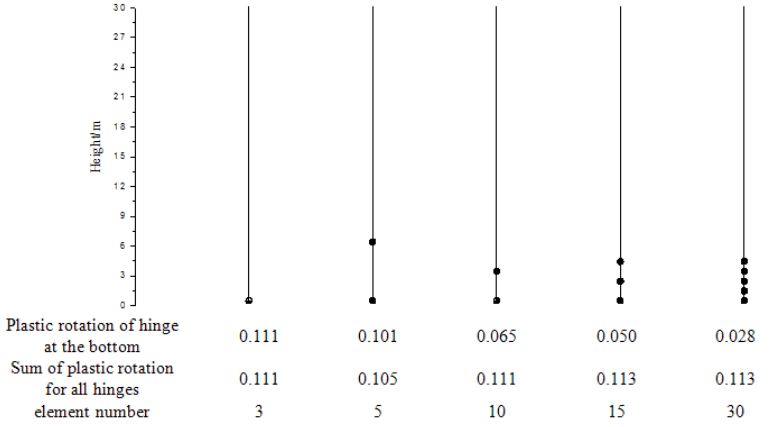

Fig. 3 Plastic hinges distribution and plastic rotation demand of 30 m pier

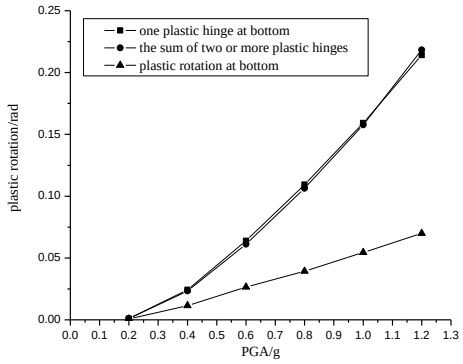

Fig. 4 Plastic rotation with different element divisions

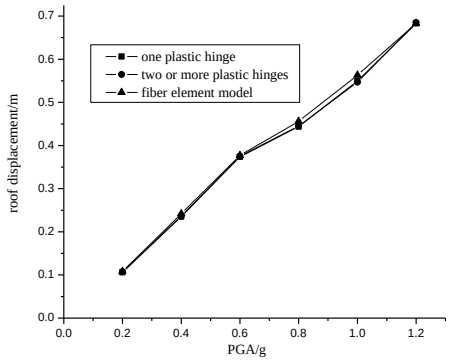

Fig. 5 Top displacement by different models

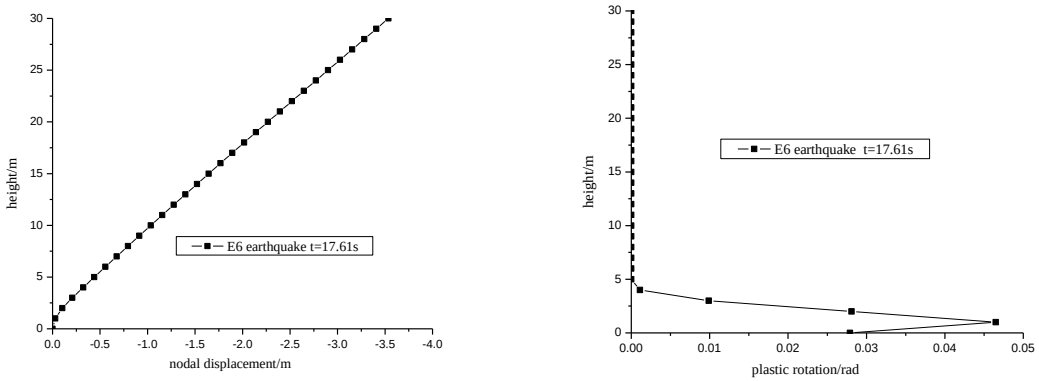

(a) maximum nodal displacement (b) maximum plastic rotation

Fig. 6 Maximum nodal displacement and plastic rotation of 30m pier

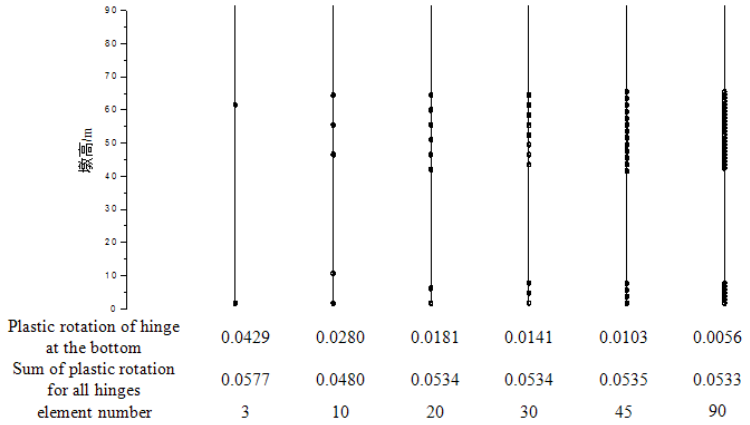

Fig. 7 Plastic hinges distribution and plastic rotation demand of 90 m pier

reaches its maximum value, respectively. From Fig. 6, it is can be seen that the displacements are generally in phase up the height of the pier.

3.2 Tall pier

For the 90 m pier, the plastic rotation demand estimated by the elastic-plastic element model with different elements subject to E6 earthquake is shown in Fig. 7. Two plastic zones were in the middle and bottom region of the pier height and indicated that the higher vibration mode contribution.

The average plastic rotation estimated by the elastic-plastic element mode with various element division subjected to 12 earthquakes scaling PGA from 0.2 g to 1.2 g is shown in Fig. 8.

From Fig. 7 and Fig. 8, the sum of the plastic rotation estimated by the elastic-plastic element mode with 3 elements was slightly different from the sum of the plastic rotation with 90 elements. Like a lower pier, if the plastic rotation for the plastic hinge at bottom of the pier is considered as plastic rotation of a tall pier, the plastic rotation demand of the pier will be underestimated overly.

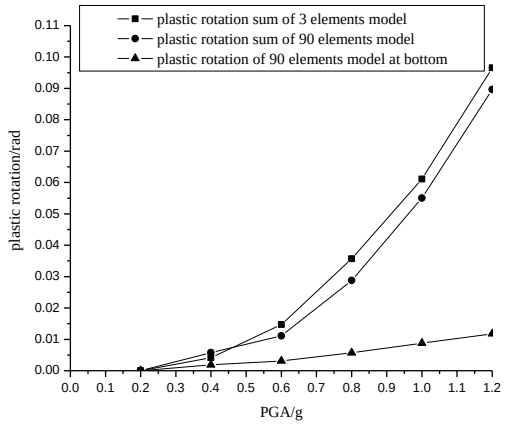

Fig. 8 Plastic rotation with different element divisions

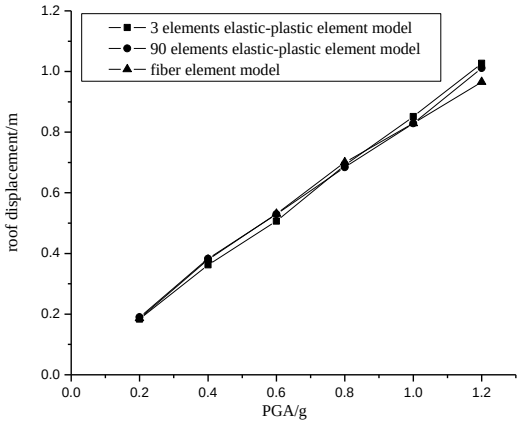

Fig. 9 Top displacement by different models

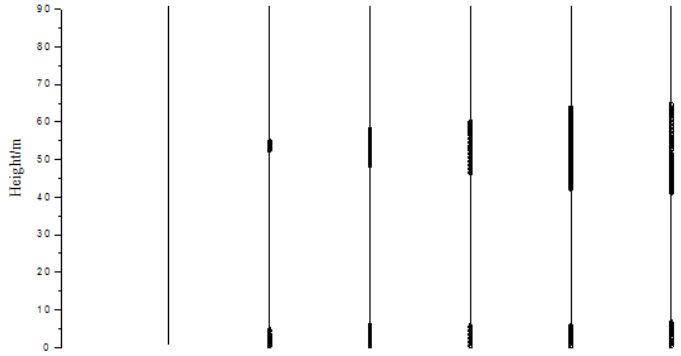

Plastic rotation of hinge at the bottom	0.0000	0.0019	0.0022	0.0034	0.0044	0.0056
Sum of plastic rotation for all hinges	0.0000	0.0058	0.0090	0.0199	0.0346	0.0533
PGA	0.2 g	0.4 g	0.6 g	0.8 g	1.0 g	1.2 g

Fig. 10 Plastic hinge formation and plastic zone expansion of 90 m pier

The average displacement at the top of the pier estimated by the elastic-plastic beam-column element with different elements and the elastic-plastic fiber beam-column element subjected to 12 earthquakes scaling PGA from 0.2 g to 1.2 g is shown in Fig. 9. From Fig. 9, it can be seen that the displacement at the top of the pier with different analytical models are almost equivalent, even for analytical model with 3 elements. The difference of displacement by elastic-plastic element model and fiber element model is about 6%~7%.

For a tall pier, the multiple plastic hinges appear in the middle and bottom region of the pier height and the development of plastic region, magnitude of the plastic rotation as an earthquake excitation increase (E6 earthquake wave PGA be scaled from 0.2 g to 1.2 g) is shown in Fig. 10. From Fig. 10, it can be seen that as earthquake excitation increase, the plastic zone at bottom development upwards and the plastic zone in middle region of pier expands towards upwards and downwards.

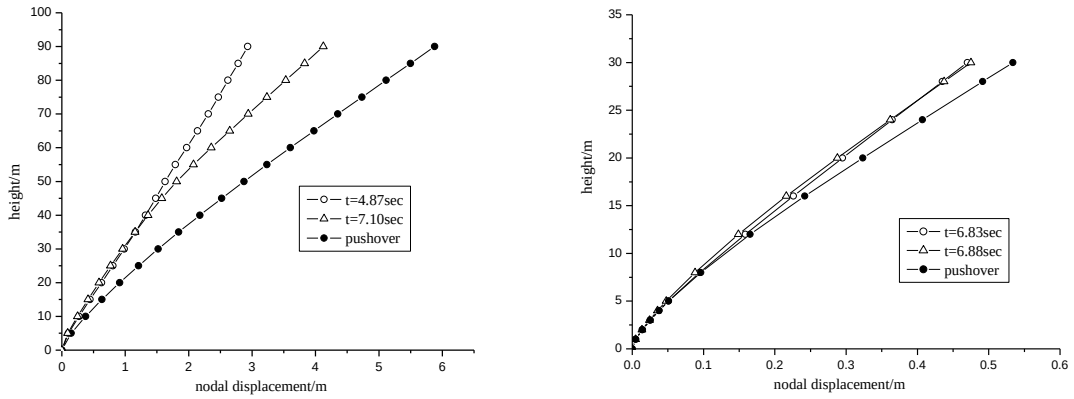

(a) 90m pier (b) 30m pier

Fig. 11 Nodal displacement

4. Local displacement capacity

In determination of local displacement capacity, empirical equations are presented for bridges suffering a minor or moderate earthquake action, while pushover analysis is proposed for bridges suffering an intensive earthquake action and considered to be a reliable and warranted method. However, the validity of both the empirical equations and the pushover analysis are based on a very important assumption that there is a one-to-one relationship between the curvature reaction at the bottom section and the lateral displacement at the top of a pier. Only one plastic hinge will occur at the bottom section and when the curvature at the bottom section reaches the ultimate value, the lateral displacement at the top also reaches the maximum value. However, this may be untenable for tall piers due to the higher modes effect.

Fig. 11(a) plots a series of instantaneous horizontal displacement values estimated by dynamic model for the 90 m height pier at 4.87 s when the curvature of bottom section reaches the ultimate state and at 19.11 s when the horizontal displacement at the top of the pier reaches its maximum, respectively. Similarly, the plots for the 30 m height pier are also shown in Fig. 11(b). It can be seen that the displacement at the top of the pier and the curvature at the bottom are out of phase for tall piers; they reach their maximum values at different instant of time. While the 30 m height pier shows quite synchronous results between the displacement at the top and the curvature at the bottom. Moreover, the curvature and horizontal displacement values estimated by static pushover analysis are also drawn in these figures. It can be seen that the local displacement capacity estimated by pushover analysis is much larger than the maximum lateral displacement at the top estimated by time-history analysis for 90 m height pier, while they are quite consistent for the 30 m height pier. This can be attributed to the higher modes effect that makes the one-to-one relationship between the curvature reaction at the bottom section and the lateral displacement at the top of a tall pier not untenable. Consequently, pushover analysis can not give a precise result on the local displacement capacity.

5. Conclusions

In this paper, nonlinear dynamic history analysis was conducted to investigate seismic demand for tall piers. The results show that:

• When there are multiple plastic hinges along a pier under an earthquake, the sum of the plastic rotation for all plastic hinges should be represented the seismic plastic rotation demand for a pier. If the plastic rotation for plastic hinge at bottom of a pier is considered as the plastic rotation demand of the pier, it will be underestimated overly.

• For tall piers, two plastic zones may form in the middle and bottom region of the pier height due to higher modes contribution. As earthquake excitation increase, the plastic zone at bottom develops upwards and the plastic zone in middle region of pier develops towards upwards and downwards.

• Because of the higher modes effect, the one-to-one relationship between the curvature reaction at the bottom section and the lateral displacement at the top becomes untenable for a tall pier. Thus pushover analysis can not appropriately predict the local displacement capacity for a tall pier.

Acknowledgments

The research reported in this paper was funded by the National Key Basic Research Program of China (2013CB036302), the National Natural Science Foundation of China (51378384), and the Fundamental Research Funds for the Central Universities (20113184). This support is gratefully acknowledged.

References

AASHTO (2007), AASHTO Guide Specification for LRFD Seismic Bridge Design, Washington, D.C.

Bresler, B. and Pister, K.S. (1985), "Strength of concrete under combined stresses", *ACI J*, **551**(9), 321-345.

Bu, Z.Y., Ding, Y., Chen, J. and Li, Y.S. (2012), "Investigation of the Seismic performance of precast segmental tall Bridge columns", *Struct. Eng. Mech.*, **43**(3), 287-309.

Ceravolo, R., Demarie, G.V., Giordano, L., Mancini, G. and Sabia, D. (2009), "Problems in applying code-specified capacity design procedures to seismic design of tall piers", *Eng. Struct.*, **31**(8), 1811-1821.

Fan, L.C. (2007), "Life cycle and performance based seismic design of major bridges in China", *Front. Arch. Civil Eng. China*, **1**(3), 261-266.

Gould, P.L. and Huang, W. (2006), "Higher mode effects in the nonlinear static analysis of a collapsed chimney", *Proceedings of the 2006 Structures Congress*, Missouri, May.

JTG/T B02-01-2008 (2008), Guidelines for Seismic Design of Highway Bridges, Beijing.

Kowalsky, M.J. (2000), "Deformation limit states for circular reinforced concrete bridge column", *J. Struct. Eng*., ASCE, **126**(8), 869-878.

Li, J.Z., Song, X.D. and Fan, L.C. (2005), "Investigation for displacement ductility capacity of tall piers", *Earthq. Eng. Eng. Vib.*, **25**(1), 43-48.

Mander, J.B., Dhakal, R.P., Mashiko, N. and Solberg, K.M. (2007), "Incremental dynamic analysis applied to seismic financial risk assessment of bridges", *Eng. Struct.*, **29**(10), 2662-2672.

Mander, J.B., Priestley, M.J.N. and Park, R. (1988), "Theoretical stress-strain model for confined concrete", *J. Struct. Div.*, ASCE, **114**(8), 1804-1826.

Memari, A.M., Harris, H.G., Hamid, A.A. and Scanlon, A. (2010), "Seismic evaluation of an elevated

highway bridge in a low seismic region - a case study", *Open Civil Eng. J.*, **4**, 72-87.
Mohd, Y.M.Y. (1994), "Nonlinear analysis of prestressed concrete structures under monotonic and cyclic loads", Ph.D. Dissertation, University of California, Berkeley.
Poursha, M., Khoshnoudian, F. and Moghadam, A.S. (2009), "A consecutive modal pushover procedure for estimating the seismic demands of tall buildings", *Eng. Struct.*, **31**(2), 591-599.
Priestley, M.J.N., Seible, F. and Calvi, G.M. (1996), *Seismic Design and Retrofit of Bridges*, John Wiley & Sons, New York, NY, USA.
Priestley, M.J.N., Calvi, G.M., and Kowalsky, M.J. (2007), *Displacement-Based Seismic Design of Structures*, IUSS Press, Pavia, Italy.
Silvia, M., Frank, M., Michael, H. (2005), *Open System for Earthquake Engineering Simulation User Manual*, Pacific Earthquake Engineering Research Center, University of California, Berkeley, CA, USA.
Taucer, F.F. and Enrico, S.F. (1991). *A Fiber Beam-Column Element for Seismic Response Analysis of Reinforced Concrete Structures*, UCB/EERC-91/17, Berkeley.
Tsai, M.H. and Chang, K.C. (2002), "Higher-mode effect on the seismic responses of buildings with viscoelastic dampers", *Earthq.Eng.Eng.Vib.* **1**(1), 119-129.
Vmvatsikos, D. and Cornell, C.A. (2002), "Incremental dnamic aalysis", *Earthq.Eng.Struct.Dyn.* **31**(3), 491-514.